9058 *Macromolecules* **2009**, *42*, 9058–9062
DOI: 10.1021/ma901591r

Macromolecules
ARTICLE

The Plumber's Nightmare Phase in Diblock Copolymer/Homopolymer Blends. A Self-Consistent Field Theory Study.

Francisco J. Martinez-Veracoechea and Fernando A. Escobedo*

School of Chemical and Biomolecular Engineering, Cornell University, Ithaca, New York 14853

Received July 20, 2009; Revised Manuscript Received August 29, 2009

ABSTRACT: Using self-consistent field theory, the Plumber's Nightmare and the double diamond phases are predicted to be stable in a finite region of phase diagrams for blends of AB diblock copolymer (DBC) and A-component homopolymer. To the best of our knowledge, this is the first time that the P phase has been predicted to be stable using self-consistent field theory. The stabilization is achieved by tuning the composition or conformational asymmetry of the DBC chain, and the architecture or length of the homopolymer. The basic features of the phase diagrams are the same in all cases studied, suggesting a general type of behavior for these systems. Finally, it is noted that the homopolymer length should be a convenient variable to stabilize bicontinuous phases in experiments.

Introduction

Diblock copolymer (DBC) systems present the attractive feature that under the appropriate conditions they self-assemble in periodical nanomorphologies that can be exploited in a vast number of technological applications.[1] One of the most attractive families of morphologies, the so-called ordered bicontinuous structures,[2] has potential applications in the fabrication of highly porous materials,[3−5] high-conductivity nanocomposites,[6] 3D photonic crystals,[7] and efficient dye-sensitized solar cells.[8,9] Unfortunately, bicontinuous behavior can be obtained only in a narrow region of the pure DBC phase diagram.[10] Moreover, while some surfactant systems have shown a wide variety of bicontinuous structures like the gyroid (G) phase, the double-diamond (DD) phase, the Plumber's Nightmare phase (P), the Neovius [C(P)] phase, etc.;[11,12] in the pure DBC system the G phase is the only stable bicontinuous morphology.[10,13,14] In addition, recent studies have predicted[14,15] and observed,[16,17] in an even narrower region of the DBC phase diagram, the cocontinuous network O^{70} phase.

The traditional explanation for the limited stability in DBC systems of the bicontinuous phases is the existence of packing frustration inside their nodes.[18] In this type of phases, the minority component forms two independent networks, each of which is composed by tubes (connectors) and nodes (where several tubes meet). When the interface between the minority (A) and majority (B) components approaches the constant-mean-curvature surface that would minimize interfacial energy, the nodes become bulkier than the tubes.[19] Thus, as the chains try to fill the space inside the nodes, they encounter an entropically unfavorable scenario (i.e., packing frustration) which may entail such effects as chain stretching, appearance of lower density regions, and deformation of the nodal shape.[20,21] The larger the number of tubes that merge in a node, the bulkier the node, and therefore the greater the entropic penalty.[18] While the G phase only has three tubes meeting in each node, the DD and P phases have four and six tubes per node, respectively,[22] therefore justifying the lack of stability of the latter phases in the pure DBC melt.

It has been argued that alleviation of packing frustration could be used to allow the stabilization of multiple bicontinuous phases.[18,19,23,24] One such strategy is the use of DBCs with chain-length dispersity;[19] in this case, longer chains could concentrate in the nodes and therefore avoid chain stretching. Although this strategy has been shown, both in simulations[20] and experiments,[25] to induce the formation of the G phase in areas of the phase diagram where it was not previously stable; little evidence exists that it can be used to stabilize any bicontinuous phase other than the G phase.[24,26] An alternative strategy for reducing packing frustration, is the addition of a selective-filler that has affinity for the A component.[18] Indeed, the stabilization of the P phase by addition of an inorganic aluminosilicate with affinity for one of the blocks has been reported in experimental work[27,28] (note, however, that one of these systems was recently re-examined and reclassified as a "distorted" gyroid[29]). Particle-based simulations (PBS) in DBC and triblock copolymers,[23,30] have shown that adding A-component homopolymer (A−Ho) can indeed lower the free energies of the DD and P phases, because the Ho concentrates inside the nodes, and hence, packing frustration is reduced. Moreover, self-consistent field theory (SCFT) calculations have predicted the stabilization of the DD phase in DBC melts by addition of A-component homopolymer.[31,32] However, addition of A−Ho to DBC melts has the additional complication that the system can macrophase separate into a DBC-rich phase and a homopolymer-rich (HoR) phase,[33,34] thus limiting the achievable range of Ho concentrations.

One shortcoming of PBS is that macrophase separation can be precluded by the relatively small simulation boxes that are used for computational tractability.[32,35] While specialized simulation methods could be used that explicitly assume a two-phase state, they are nontrivial to implement with bicontinuous phases for which the box size is a key parameter that needs to be found by trial and error. In order to overcome this difficulty, in a previous work[32] we used a combination of PBS and SCFT to study the stabilization of bicontinuous phases in DBC systems by the addition of linear A−Ho of the appropriate length. The SCFT calculations showed that although the DD phase could be stable in a significant region of the phase diagram, the P phase was always metastable with respect to macrophase separation at the conditions studied. Clearly, achieving the stabilization of multiple bicontinuous phases entails more than just alleviating packing frustration: it also requires circumventing macrophase separation.

*Corresponding author. E-mail: fe13@cornell.edu.

 Published on Web 09/11/2009

In our previous work[32] we found that, though always metastable, the P phase could be nearly stable in some regions of the phase diagram studied. Therefore, in the present work we use SCFT in order to study the effect on the stabilization of the P phase of distinct system parameters; namely, the volume fraction (f) of the A-block relative to the total DBC chain, the use of a four-arm-star architecture instead of a linear one for the A−Ho, and the relative length $\alpha = N_{ho}/N_{DBC}$ of the linear A−Ho.

Methodology

SCFT has been widely used previously in the study of block copolymer systems and details about its implementation can be found elsewhere.[36,37] In particular, studies of DBC/homopolymer blends have been carried out successfully in previous theoretical works.[31−33] In the present article we used a slightly modified version of the code developed by Morse, Tyler, and coworkers[38−42] to solve the self-consistent equations. We used the Canonical (NVT) ensemble together with the matching of the (zero pressure[43]) chemical potentials of each specie in the two different phases to calculate macrophase coexistence. This approach is equivalent to the Grand Canonical approach commonly used by previous authors.[37,44] Finally, a number of up to 80 grid points were used in each direction to ensure enough accuracy in the solution of the SCFT equations.

Results

For a pure DBC system at a given value of χN, the value of f determines the curvature of the observed morphology. While the minimization of the interfacial energy tends to reduce the A−B interfacial area, the maximization of the chains' conformational entropy and the constraint of incompressibility tend to curve the A−B interface toward the short-chain domains. The interplay of these two opposite tendencies determines the final morphology, and results in the familiar sequence of structures observed as f increases (from 0 to 0.5) in the intermediate segregation regime of the pure DBC melt: disorder → spheres → cylinders (C) → G → lamellar (L). In a previous study,[32] we showed that the phase diagram of DBC/A−Ho blends with $\alpha = 0.80$ was very sensitive to the exact value of f. For example, it was seen that while for $f = 0.325$ only the C and G phases were stable, for $f = 0.33$ the DD phase (in addition to the G and C phases) was fully stable in a significant region of phase diagram. The P phase, however, was always found metastable with respect to macrophase separation.

In order to thoroughly examine whether there exists a range of values of f wherein the P phase is fully stable, we use SCFT to calculate the phase diagram of a DBC/A−Ho blend with $\alpha = 0.80$ and $\chi N = 25$, and present it in Figure 1 as a plot of f versus ϕ_{ho} (Ho volume fraction). The resulting phase diagram shows that both the DD and P phases are fully stable in finite regions of the phase diagram. This is (to the best of our knowledge) the first study where the P phase has been theoretically predicted to be fully stable in a block copolymer-containing system. The gray areas in the diagram indicate two-phase coexistence between adjacent mesophases or between one mesophase and the homogeneous HoR phase. Throughout this work the HoR phase reported is always almost pure Ho since $\phi_{ho} > 0.99999$ at all the conditions examined. Triple points among the different phases are indicated with dash lines. Note that as the value of f where the C-G transition occurs in the pure system is approached (i.e., $f = 0.3258$), two azeotropes between the C and G phases are observed. At high values of f (i.e., $f > 0.3362$), coexistence between the G and L phases also starts in an azeotrope.

Though the region where the P phase is fully stable as a single phase is considerably narrow, the regions where the P phase is in equilibrium either with the G or DD phases are considerably wider, indicating that a mixture of two bicontinuous phases could in principle be more attainable. Moreover, given that both the DD and P phases are in equilibrium with the HoR phase (and that the corresponding two-phase gray area in Figure 1 extends up to $\phi_{ho}\sim1$), one possible strategy to obtain these phases experimentally could involve adding an excess of Ho and just collecting them as the product of the phase separation. The efficacy of this approach, however, could be limited by the kinetics of macrophase separation.

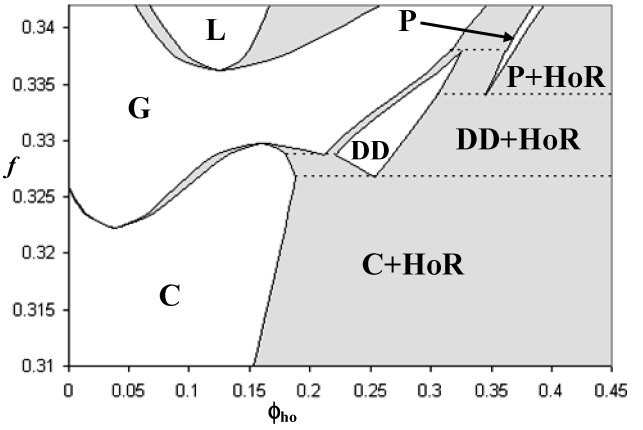

Figure 1. Phase diagram of a DBC/A−Ho blend in which the A-block volume fraction in the DBC (f) is shown as a function of the Ho volume fraction (ϕ_{ho}) at $\chi N = 25$ for $\alpha = 0.80$. The single phase regions are shown in white while coexistence regions are presented in gray. Triple points are indicated with dashed lines.

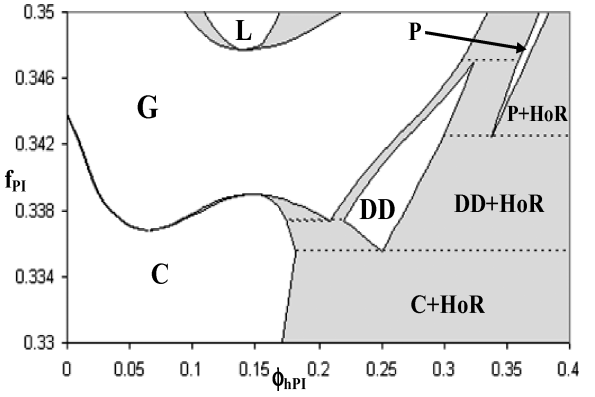

Figure 2. Phase diagram of a PI-*b*-PS/hPI blend in which the PI-block volume fraction f_{PI} is presented as a function of the hPI volume fraction (ϕ_{hPI}) at $\chi N = 25$ for a hPI size of $\alpha = 0.80$.

In real DBC systems there always exists conformational asymmetry between the DBC blocks (i.e., the statistical segment lengths a_i of the two blocks are not equal).[45] This asymmetry have been shown[46] to shift the observed phase diagram, because the A−B interface tends to curve toward the component with the longer statistical segment length. Considering the sensitivity of the observed diagram to the value of f in DBC/Ho blends, we investigated the effect of conformational asymmetry in the stabilization of bicontinuous phases. We chose as a test case the values corresponding for a blend of PI-*b*-PS and PI-homopolymer (hPI), wherein the statistical segment length ratio between PI and PS is given by[47] $a_{PI}/a_{PS} = 1.11$. In Figure 2, we present the predicted phase diagram for this system at $\chi N = 25$ and $\alpha = 0.80$, in a plot of f_{PI} against the volume fraction of hPI (ϕ_{hPI}). Expectedly, the predicted phase behavior is qualitatively similar to the one observed for the conformationally symmetric case (Figure 1), the major difference being that the C−G transition in the pure system ($f_{PI} = 0.3438$), and with it the whole phase diagram, has been shifted to higher values of f.

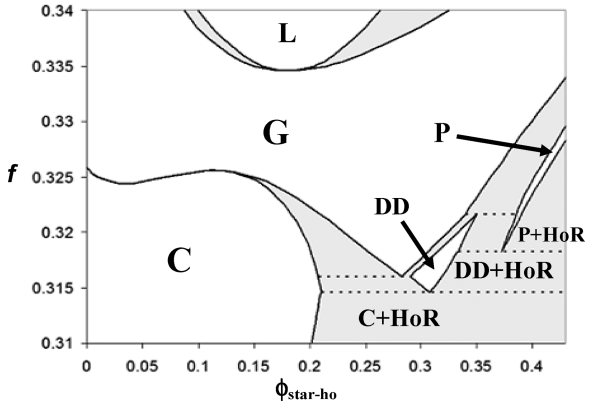

Figure 3. SCFT phase diagram (f versus $\phi_{star\text{-}ho}$) of a model DBC/star-Ho blend at $\chi N = 25$. The star-Ho has four arms of length $\alpha_{arm} = 0.20$ each.

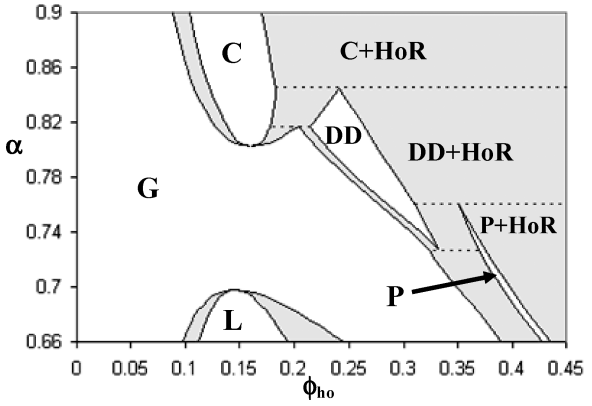

Figure 4. DBC/Ho phase diagram in which the Ho length (α) is plotted as a function of ϕ_{ho} at $\chi N = 25$ and $f = 0.33$.

The fact that the HoR phase is to a very good approximation pure Ho ($\phi_{ho} > 0.99999$) implies that the value of ϕ_{ho} at which the DBC-rich phase coexists with the HoR phase is mostly determined by the A−Ho chemical potential. Hence, macrophase separation can be "pushed" toward higher values of ϕ_{ho} by lowering (at a given value of ϕ_{ho}) the Ho chemical potential in the DBC-rich phase with respect to that of the pure Ho. Indeed, for the sizes of Ho considered above, the Ho chains are effectively confined to the A-domain region, hence, forcing the linear chains to adopt more compact structures and therefore raising their chemical potential.[23] However, the Ho architecture can be changed to favor more compact conformations (e.g., branched or ring-shaped Ho), thus reducing the entropic penalty under confinement and increasing the Ho solubility in the DBC-rich phase. To test this idea, we studied a (conformationally symmetric) DBC/star-Ho blend where the star-Ho is composed of four arms of length $\alpha_{arm} = 0.20$ each (total contour length $\alpha_{tot} = 0.80$), which can be directly compared with the linear Ho case. We present the SCFT phase diagram of this model system at $\chi N = 25$ in Figure 3, in a plot of f versus volume fraction of star-Ho ($\phi_{star\text{-}ho}$). As anticipated, the $\phi_{star\text{-}ho}$ at which the DBC-rich phases coexist with the HoR phase are shifted to higher values. In addition, the appearance of the DD and P phases is displaced to lower values of f than in the linear-Ho case. However, the thickness of the pure P-phase stability region is unchanged and the general features of the phase diagram (i.e., sequence of phases and topology) remain remarkably similar to those of the phase diagrams shown before, suggesting that the stabilization of the DD and P phases is more or less independent to the exact details of the DBC/Ho system under consideration.

For the A−Ho and A-block lengths studied above (i.e., $\alpha = 0.80$ and $0.31 \leq f \leq 0.35$, respectively), or equivalently, for values of the Ho-to-A-block length ratio $\gamma \equiv N_{\text{Ho}}/N_{\text{A-block}} = \alpha/f$ in the range $2.29 \leq \gamma \leq 2.58$, the Ho is not expected to significantly penetrate into the A-*block*-rich region (dry brush regime, $\gamma > 1$),[1] therefore inducing the formation of phases of *more* interfacial curvature like the DD and P phases,[23,48] but also risking macrophase separation into a DBC-rich phase and a HoR phase.[33] Conversely, if $\gamma < 1$, the Ho will swell the affine (A) block (wet brush regime[1]), preventing macrophase separation, but inducing phases of *less* interfacial curvature (e.g., L, reverse G, reverse C, etc.), instead of the desired bicontinuous phases.[48] However, for intermediate values of γ in between these two extreme cases, there might exist a region of phase diagram where inducing bicontinuous phases and circumventing macrophase separation can be both achieved. For this purpose we examined the case where $f = 0.33$ and $\chi N = 25$, wherein it was shown previously that a transition of the form G → DD could be induced by addition of A−Ho with $\alpha = 0.80$, but where the P phase was always found metastable.[32] In Figure 4, we present the phase diagram for the DBC/A−Ho blend in the space of α vs ϕ_{ho}. For the pure system (i.e., $\phi_{ho} = 0$) the G phase is stable. The immediate feature to notice is that the P phase starts being stable for values of $\alpha < 0.7596$, where a triple-point between the DD, P, and HoR phases is located. Another remarkable feature, is that the shape of the high-ϕ_{ho} region of the phase diagram shown in Figure 4, is the same as the one observed in the high-ϕ_{ho} region of Figure 1 (except that it is displayed upside down), indicating that the effect of increasing the value of f (at fixed α) is analogous to that of decreasing α (at fixed f). The physical basis for this analogy is that either of these two actions reduces the tendency of the Ho to separate out as a HoR phase, thus allowing the DD and P phases to be stable as single phases. Though this phase behavior would seem to suggest that the relevant quantity for determining morphology stability is the ratio γ; such a relevance is only qualitative. Indeed, in Figure 1 f is varied in the narrow range $0.31 \leq f \leq 0.342$, a ∼10% change in γ, while in Figure 4 the Ho size needs to be varied over a much wider range $0.66 \leq \alpha \leq 0.90$, a ∼ 35% change in γ, in order to observe similar mesophases. This weaker dependence of the phase behavior upon α can prove beneficial, since it would provide a much more practical means to experimentally control phase transitions between distinct morphologies.

Interestingly, as one decreases the value of α the system goes through a series of triple points between the mesophases and the HoR phase. At $\alpha = 0.8448$ there is a C-DD-HoR triple point which marks the beginning of the region of stability of the DD phase; then at $\alpha = 0.7596$ a DD-P-HoR triple point occurs that signals the start of the P phase region. Therefore, it is possible that at even lower values of α, new triple points exist that will start the regions of stability of other bicontinuous phases like the C(P) or the I-WP phases, in a similar sequence as that observed in some related surfactant systems.[11,12] These phases, however, would have unit cells much larger than our current computational capabilities can handle and are outside the scope of the present work.

In order to emphasize the importance of the effect of α in stabilizing a given bicontinuous morphology we show in Figure 5 a plot of the difference in Helmholtz free energy ($\beta\Delta F$) of the DD and P phases with respect to the G phase, as a function of α. In Figure 5a ($\phi_{ho} = 0.30$) the G phase has the lowest free energy for low values of α, but as the value of α increases, the DD phase and then the P phase are seen to have the lowest free energy. Nevertheless, the P phase is never fully stable at these conditions, since the system first undergoes macrophase separation in DBC-rich and HoR phases (dashed line). In Figure 5b ($\phi_{ho} = 0.38$) a direct transition from the G phase to the P phase is observed with

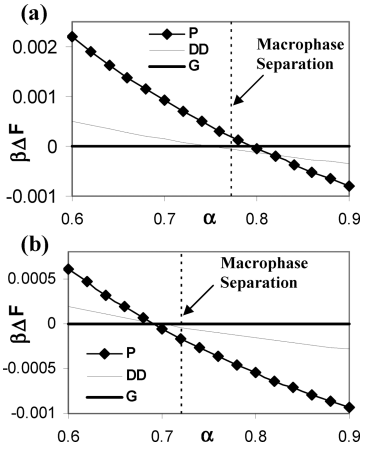

Figure 5. Difference in Helmholtz free energy ($\beta\Delta F$) between distinct phases and the G phase as a function of α for the DBC/Ho system at $\chi N = 25$ and $f = 0.33$. The dashed line indicates the point at which macrophase separation occurs. (a) The homopolymer concentration is $\phi_{ho} = 0.30$. (b) The homopolymer concentration is $\phi_{ho} = 0.38$.

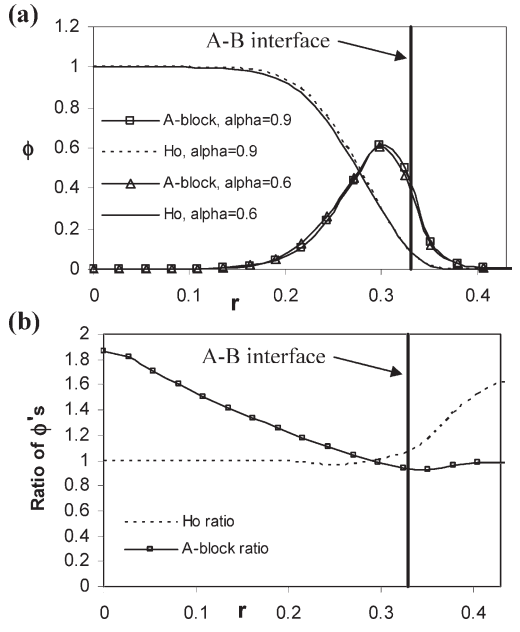

Figure 6. Volume fraction profiles of the A-blocks and the Ho chains as a function of the distance from the center of the P phase node in the 111 direction, for two different cases (i.e., α = 0.6 and α = 0.9). (a) The absolute values of the volume fractions are plotted. The center of the node is essentially pure homopolymer. (b) The ratio of the volume fractions between the α = 0.6 case and the α = 0.9 case are shown. In the system with shorter Ho-chains there is more mixing between homopolymers and A-blocks.

increasing values of α. Again the dashed line represents the point where the system undergoes macrophase separation.

In Figure 6, we analyze the A-block and homopolymer's volume fraction (ϕ) profile in the (111) direction (i.e., the diagonal of the unit cell) as a function of the distance (r) from the center of the P phase' node (r is normalized by the length of the unit cell edge). The total homopolymer volume fraction is $\phi_{ho} = 0.30$ and we compare the two linear homopolymer lengths in the extremes of the range studied in the present work (i.e., α = 0.9 and α = 0.6.). Although the P phase is metastable at these conditions, this comparison is meant to probe the effect of α on homopolymer spatial distribution inside nodes of the same morphology. In Figure 6a, we show the homopolymer's and A-block's volume fractions as functions of r. The solid vertical line indicates the location of the A−B interface (i.e., where $\phi_A = \phi_B = 0.5$). As expected for this range of homopolymer lengths (i.e., $\gamma > 1$), the homopolymer is essentially pure in a significant region at center of the node while its concentration decreases rapidly as the interface is approached. Conversely, the A-block volume fraction reaches a maximum in the proximity of the interface, thus showing that the A-block and homopolymer chains are spatially segregated with little mixing between them. These observations are consistent with the hypothesized mechanism of packing frustration relief and with previous results reported using PBS.[23] While Figure 6a shows that the concentration profiles are essentially the same for α = 0.9 and α = 0.6, their differences are amplified in Figure 6b by plotting the ratio of the volume fractions between the α = 0.6 case and the α = 0.9 case. That is, we plot the Ho ratio $\phi_{ho}|_{\alpha = 0.6}/\phi_{ho}|_{\alpha = 0.9}$ and the A-block ratio $\phi_{A\text{-}block}|_{\alpha = 0.6}/\phi_{A\text{-}block}|_{\alpha = 0.9}$ as a function of r. Figure 6b shows that the Ho ratio is essentially unity in the node interior ($r \sim 0$), begins to increase in the proximity of the interface, and becomes significantly larger than one after crossing the interface. This indicates that the shorter homopolymer chains (i.e., α = 0.6) have a greater tendency to penetrate toward the interfacial region than the longer ones, as expected from mixing-entropy considerations. The A-block ratio is unity close to the interface and increases as the node center is approached; this shows that the A-blocks of the α = 0.6 case have a slightly larger tendency to reach toward the node center and to mix with the Ho chains than the A-blocks of the α = 0.9 case. While these differences are very small in terms of absolute concentration values, they reflect underlying free-energy differences that can be of crucial importance for the stability of a particular phase, as can be seen in the pronounced effect that changes in α can have in the predicted DBC/homopolymer phase diagram (cf., Figures 4 and 5).

Conclusions

We have used SCFT to study the effect that different system parameters have in the stabilization of the DD and P phases in DBC/Ho blends. In particular, we studied the effect of variations in: the A-block size (f), the A−B asymmetry, the Ho architecture and the Ho length (α). The DD and P phases were both found to be stable in finite regions of the calculated phase diagrams. To the best of our knowledge, this is the first time that the P phase has been predicted to be stable using SCFT. Interestingly, in the f versus ϕ_{ho}, diagrams, the basic features of the phase behavior were found to be largely insensitive to variations of conformational asymmetry (PI-*b*-PS case) and architecture (star-Ho case), suggesting that this kind of phase behavior is essentially independent of the specific features of the particular DBC system studied. Additionally, the resemblance of the high-ϕ_{ho} phase behavior observed when decreasing the Ho length (α) to the case when increasing the A-block length (f) suggests that as long as the value of f is close to the C−G transition in the pure melt, one can find a suitable value of α that will allow stabilization of the DD and P phases. It is thus argued that variation of the Ho size provides a convenient means to control the stability of complex morphologies in DBC/Ho blends. We hope that the current work will serve as a guide to experimental efforts devoted to obtaining bicontinuous phases in this type of amphiphilic systems.

Acknowledgment. We are very grateful to Prof. David Morse and his student Jian Qin for providing the code and guidance to implement the SCFT calculations. We are also grateful to Prof. U. Wiesner for helpful discussions. This publication is based on work supported in part by Award No. KUS-C1-018-02, made by King Abdullah University of Science and Technology (KAUST). Additional support from the National Science Foundation Award 0756248 is also gratefully acknowledged.

References and Notes

(1) Hamley, I. W., *The Physics of Block Copolymers*; Oxford University Press: Oxford, U.K.,1998.
(2) Andersson, S.; Hyde, S. T.; Larsson, K.; Lidin, S. *Chem. Rev.* **1988**, *88*, 221–242.
(3) Uehara, H.; Yoshida, T.; Kakiage, M.; Yamanobe, T.; Komoto, T.; Nomura, K.; Nakajima, K.; Matsuda, M. *Macromolecules* **2006**, *39*, 3971–3974.
(4) Kamperman, M.; Garcia, C. B. W.; Du, P.; Ow, H. S.; Wiesner, U. *J. Am. Chem. Soc.* **2004**, *126*, 14708–14709.
(5) Adachi, M.; Okumura, A.; Sivaniah, E.; Hashimoto, T. *Macromolecules* **2006**, *39*, 7352–7357.
(6) Cho, B. K.; Jain, A.; Gruner, S. M.; Wiesner, U. *Science* **2004**, *305* (5690), 1598–1601.
(7) Urbas, A. M.; Maldovan, M.; DeRege, P.; Thomas, E. L. *Adv. Mater.* (*Germany*) **2002**, *14* (24), 1850–1853.
(8) Crossland, E. J. W.; Kamperman, M.; Nedelcu, M.; Ducati, C.; Wiesner, U.; Smilgies, D. M.; Toombes, G. E. S.; Hillmyer, M. A.; Ludwigs, S.; Steiner, U.; Snaith, H. J., *Nano Lett.* Article ASAP. DOI: 10.1021/nl803174p.
(9) Nedelcu, M.; Lee, J.; Crossland, E. J. W.; Warren, S. C.; Orilall, M. C.; Guldin, S.; Huttner, S.; Ducati, C.; Eder, D.; Wiesner, U.; Steiner, U.; Snaith, H. J. *Soft Matter* **2009**, *5*, 134–139.
(10) Matsen, M. W.; Bates, F. S. *J. Chem. Phys.* **1997**, *106*, 2436–2448.
(11) Strom, P.; Anderson, D. M. *Langmuir* **1992**, *8*, 691–709.
(12) Schwarz, U. S.; Gompper, G. *J. Chem. Phys.* **2000**, *112*, 3792–3802.
(13) Cochran, E. W.; Garcia-Cervera, C. J.; Fredrickson, G. H. *Macromolecules* **2006**, *39*, 2449–2451.
(14) Tyler, C. A.; Morse, D. C. *Phys. Rev. Lett.* **2005**, *94*, 208302.
(15) Guo, Z. J.; Zhang, G. J.; Qiu, F.; Zhang, H. D.; Yang, Y. L.; Shi, A. C. *Phys. Rev. Lett.* **2008**, *101*, 4.
(16) Takenaka, M.; Wakada, T.; Akasaka, S.; Nishitsuji, S.; Saijo, K.; Shimizu, H.; Kim, M. I.; Hasegawa, H. *Macromolecules* **2007**, *40*, 4399−4402.
(17) Kim, M. I.; Wakada, T.; Akasaka, S.; Nishitsuji, S.; Saijo, K.; Hasegawa, H.; Ito, K.; Takenaka, M. *Macromolecules* **2008**, *41*, 7667–7670.
(18) Matsen, M. W.; Bates, F. S. *Macromolecules* **1996**, *29*, 7641–7644.
(19) Hasegawa, H.; Hashimoto, T.; Hyde, S. T. *Polymer* **1996**, *37*, 3825–3833.
(20) Martinez-Veracoechea, F. J.; Escobedo, F. A. *Macromolecules* **2005**, *38*, 8522–8531.
(21) Martinez-Veracoechea, F. J.; Escobedo, F. A. *J. Chem. Phys.* **2006**, *125*, 104907.
(22) Gozdz, W.; Holyst, R. *Phys. Rev. Lett.* **1996**, *76*, 2726–2729.
(23) Martinez-Veracoechea, F. J.; Escobedo, F. A. *Macromolecules* **2007**, *40*, 7354–7365.
(24) Schroder-Turk, G. E.; Fogden, A.; Hyde, S. T. *Eur. Phys. J. B* **2007**, *59*, 115–126.
(25) Meuler, A. J.; Ellison, C. J.; Hillmyer, M. A.; Bates, F. S. *Macromolecules* **2008**, *41*, 6272–6275.
(26) Matsen, M. W. *Phys. Rev. Lett.* **2007**, *99*, 148304.
(27) Finnefrock, A. C.; Ulrich, R.; Toombes, G. E. S.; Gruner, S. M.; Wiesner, U. *J. Am. Chem. Soc.* **2003**, *125*, 13084–13093.
(28) Jain, A.; Toombes, G. E. S.; Hall, L. M.; Mahajan, S.; Garcia, C. B. W.; Probst, W.; Gruner, S. M.; Wiesner, U. *Angew. Chem., Int. Ed. Engl.* **2005**, *44*, 1226–1229.
(29) Toombes, G. E. S.; Finnefrock, A. C.; Tate, M. W.; Ulrich, R.; Wiesner, U.; Gruner, S. M. *Macromolecules* **2007**, *40*, 8974–8982.
(30) Dotera, T. *Phys. Rev. Lett.* **2002**, *89*, 205502.
(31) Matsen, M. W. *Phys. Rev. Lett.* **1995**, *74*, 4225–4228.
(32) Martinez-Veracoechea, F. J.; Escobedo, F. A. *Macromolecules* **2009**, *42*, 1775–1784.
(33) Matsen, M. W. *Macromolecules* **1995**, *28*, 5765–5773.
(34) Mareau, V. H.; Matsushita, T.; Nakamura, E.; Hasegawa, H. *Macromolecules* **2007**, *40*, 6916–6921.
(35) Frenkel, D.; Smit, B., *Understanding Molecular Simulation.* Academic Press: San Diego, CA, 2002.
(36) Fredrickson, G., *The Equilibrium Theory of Inhomogeneous Polymers.* Oxford University Press: New York, 2006.
(37) Matsen, M. W. *J. Phys.: Condens. Matter* **2002**, *14*, R21–R47.
(38) Morse, D. C.; Tyler, C. A.; Ranjan, A.; Qin, J.; Thiagarajan, R. PSCF - Home Page. http://www.cems.umn.edu/research/morse/code/pscf/home.php
(39) Tyler, C. A.; Morse, D. C. *Macromolecules* **2003**, *36*, 8184–8188.
(40) Tyler, C. A.; Morse, D. C. *Macromolecules* **2003**, *36*, 3764–3774.
(41) Ranjan, A.; Morse, D. C. *Phys. Rev. E* **2006**, *74* (1).
(42) Ranjan, A.; Qin, J.; Morse, D. C. *Macromolecules* **2008**, *41*, 942–954.
(43) Chang, K.; Morse, D. C. *Macromolecules* **2006**, *39*, 7397–7406.
(44) Beardsley, T.; Matsen, M. *Eur. Phys. J. E* **2008**, *27*, 323–333.
(45) Bates, F. S.; Schulz, M. F.; Khandpur, A. K.; Forster, S.; Rosedale, J. H.; Almdal, K.; Mortensen, K. *Faraday Discuss.* **1994**, *98*, 7–18.
(46) Matsen, M. W.; Bates, F. S. *J. Polym. Sci., Part B: Polym. Phys.* **1997**, *35*, 945–952.
(47) Cochran, E. W.; Morse, D. C.; Bates, F. S. *Macromolecules* **2003**, *36*, 782–792.
(48) Abetz, V.; Simon, P. F. W. Phase behaviour and morphologies of block copolymers. In *Block Copolymers I*, Albetz, V. Ed.; Springer: Berlin, 2005; Vol. *189*, pp 125−212.